EVLA Memo #206

S-band Radio Frequency Interference from Geostationary Satellites

Frank Schinzel (NRAO)

July 20, 2018

A survey of EVLA S-band (2–4 GHz) radio interference from geostationary satellites is presented in this memo. The observations were carried out between 2016 and 2017 in B configuration, combining two non-overlapping surveys. The horizon-to-horizon distribution of peak power levels are presented for declinations -17.5 – +17.5°. Additionally, the switched power information was used to produce plots visualizing the spatial severity of system compression around the satellite belt. These plots can directly be used to inform scheduling decisions around the geostationary satellite belt.

1 Introduction

Downlink transmission carriers from geostationary satellites (space-to-ground) are a growing issue for ground based radio astronomy both due to an increase in transmitting satellites and due to increases in receiving bandwidths of radio telescopes. The VLA is no exception to this. The S/C-band frequency allocations for satellite downlink carriers are listed in Table 1, which was extracted from the online FCC frequency allocation table last revised on August 25, 2017 (47 C.F.R. Paragraph 2.106). To summarize this table, VLA S-band data (2–4 GHz) can be affected by satellite broadcasts at 2.025 – 2.300 GHz, 2.4835 – 2.655 GHz, and 3.100 - 4.200 GHz. Protected bands for radio astronomy and passive remote sensing are 2.655 – 2.700 GHz. At maximum occupancy, satellite emission could affect at least 67% of available S-band bandwidth.

Fortunately, the severity of interference from satellites is a strong function of the angular offset between a particular satellite and the antenna, which is governed by the primary beam of the receiving antenna and sub-reflector configuration. The typical on-axis gain at 3.0 GHz for a 25 m VLA antenna is about +57 dBi, while at 5° off axis the gain is of the order +15 dBi (-42 dB below peak). However, significant degradation can still occur if the antennas point within ∼10° of the satellite (*priv. comm. V. Dhawan*).

A significant fraction of satellites can be found along the Clarke-Belt, the zone of geosynchronous satellites. As seen from the VLA, the belt is at declination of about −5.5°. The Satellite Database maintained by the Union of Concerned Scientists [UCS (2018)] lists 531 known active geostationary satellites (1738 in total) as of 08/31/2017. The location of known, S-band transmitting, geosynchronous satellites are shown in Fig. 1. This plot most likely underestimates the true number of S-band transmitting satellites. We expect to encounter many more since there is no complete public record of active in-orbit satellite downlink frequencies. Observations of astronomical objects in the declination range of +5° to −15° are expected to be significantly degraded due to satellite transmissions. We performed on-the-fly scanning observations horizon-to-horizon between −17.5 and +17.5° declination with a separation of 2.5° between declinations. The observations presented here only provide a snapshot of the current interference environment. The interference from satellites is highly dynamic both in occupancy and sky position. The observed situation can change at any time and with no advance notice.

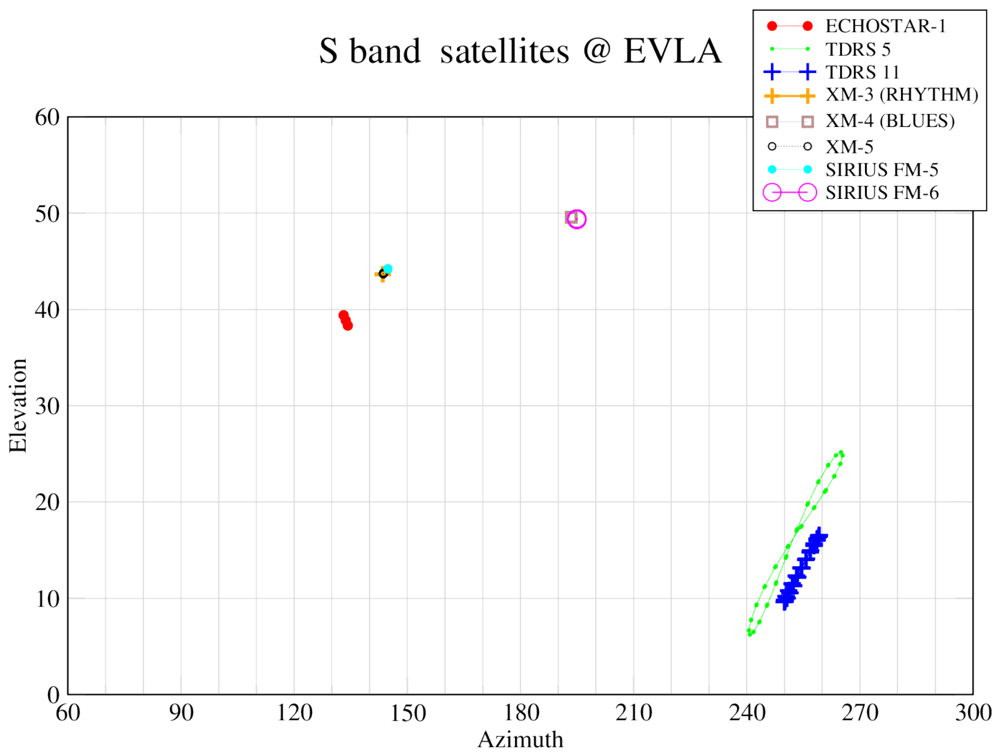

Figure 1: Known S-band transmitting satellites in geosynchronous orbit visible from the VLA. TDRS5 and TDRS11 are currently deemed inactive. *Source: V. Dhawan/D. Mertely*

Table 1: Table of Frequency allocations for space-to-Earth, space-to-space communications, and scientific use. *Source: 47 C.F.R. Paragraph 2.106 (last revised 08/25/2017)*

Frequency (GHz)	**Allocation**	**Table**
2.025 – 2.110	SPACE OPERATION (Earth-to-space) (space-to-space)	Region 1–3; Federal
	EARTH EXPLORATION SATELLITE (Earth-to-space) (space-to-space)	
	SPACE RESEARCH (space-to-space)	
2.110 – 2.120	SPACE RESEARCH (deep space) (Earth-to-space)	Region 1–3
2.120 – 2.170	Mobile-satellite (space-to-Earth)	Region 2
2.170 – 2.200	MOBILE-SATELLITE (space-to-Earth)	Region 1–3; Non-Federal
2.200 – 2.290	SPACE OPERATION (space-to-Earth) (space-to-space)	Region 1–3; Federal
	EARTH EXPLORATION-SATELLITE (space-to-Earth) (space-to-space)	
	SPACE RESEARCH (space-to-Earth) (space-to-space)	
2.290 – 2.300	SPACE RESEARCH (deep space) (space-to-Earth)	Region 1–3; Federal; Non-Federal
2.4835 – 2.50	MOBILE-SATELLITE (space-to-Earth)	Region 1–3; Federal; Non-Federal
	RADIODETERMINATION-SATELLITE (space-to-Earth)	
2.500 – 2.520	FIXED-SATELLITE (space-to-Earth)	Region 2–3
2.520 – 2.655	BROADCASTING-SATELLITE	Region 1–3
	FIXED-SATELLITE (space-to-Earth)	
2.655 – 2.690	BROADCASTING-SATELLITE	Region 1–3
	Earth exploration-satellite (passive)	Region 1–3; Federal; Non-Federal
	Radio astronomy	
	Space research (passive)	
2.690 – 2.700	EARTH EXPLORATION-SATELLITE (passive)	Region 1–3; Federal; Non-Federal
	RADIO ASTRONOMY	
	SPACE RESEARCH (passive)	
3.100 – 3.300	Earth exploration-satellite (active)	Region 1–3; Federal; Non-Federal
	Space research (active)	
3.400 – 3.700	FIXED-SATELLITE (space-to-Earth)	Region 1–3; Non-Federal
3.700 – 4.200	FIXED-SATELLITE (space-to-Earth)	Region 2–3; Non-Federal

2 Results

2.1 Observations

Two on-the-fly (OTF) observations were conducted in B array configuration. The first one was executed on September 08, 2016 under the TSKY0001 project (scheduling block id: 32701459; duration: 4 hours). This observation covered horizon-to-horizon (to about 20° elevation above horizon) and a declination range of $-10.0°$ to $7.5°$. The second observation was executed on November 08, 2017 (scheduling block id: 34669707; duration: 2 hours). This observation augmented the first one and covered declination ranges $-17.5°$ – $-12.5°$ and $10.0°$ – $17.5°$. In both cases 3C 48 was observed in an area of the sky which was not affected by satellite transmission at the beginning of the observation. Attenuators and system power levels were set in those parts of the sky. In Fig. 2 OTF tracks from the combined datasets are shown. The point at declination $+33°$ is the location of 3C 48 in the first dataset. The frequency setup was in both cases that of the VLA sky survey, covering 1.965 – 2.989 GHz. This places the frequency range 2.093 – 2.477 GHz in three separate spectral windows covering a majority of the satellite downlink bands at the lower end of the band. The lowest spectral window (1.965 – 2.093 GHz) is expected to be free of orbiting satellite interference.

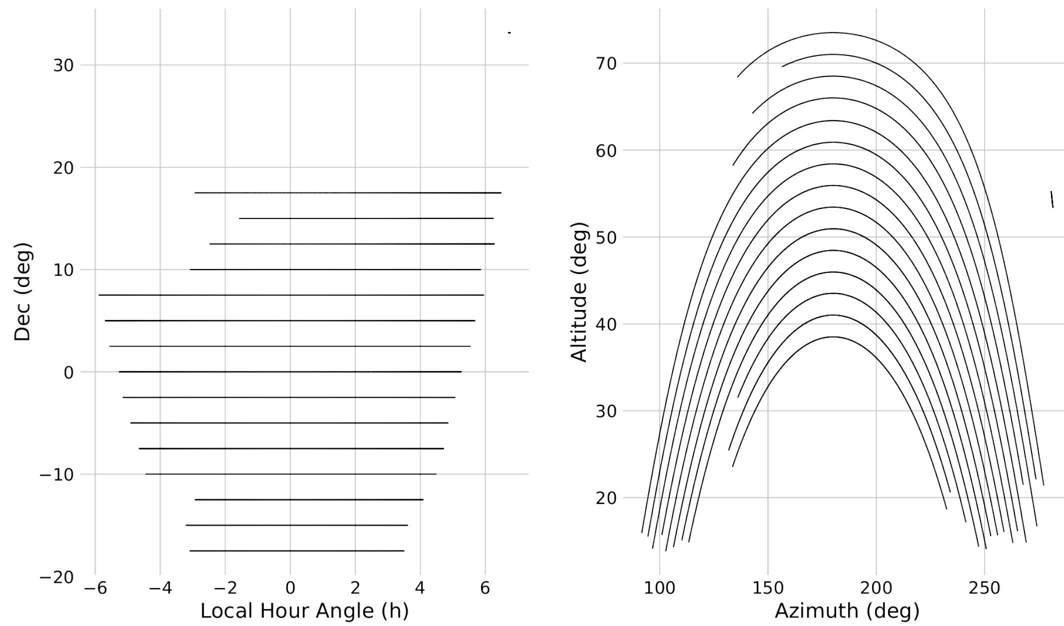

Figure 2: Combined OTF tracks of the two RFI survey observations from September 08, 2016 and November 08, 2017.

2.2 Analysis Procedure

The analysis is based on a python Jupyter notebook developed by Casey Law[1], which code was partially reused and adapted to work with *sdmpy*[2] developed by Paul Demorest. The original analysis scripts only included visualization of peak visbility amplitude values from both polarizations combined as a function of sky position and spectral window. This was expanded to include visualization of the switched power Pdiff values recorded alongside the visibilities on a per spectral window basis. The Pdiff values are normalized on a per-spectral-window, per-antenna basis, with outlier exclusion to the values observed around 3C 48 and then averaged across all antennas, resulting in one value per two integrations per spectral window. All analysis scripts directly act on the SDM/BDF dataset and do not require the generation of a measurement set or UV FITS file. All scripts can be found here `https://github.com/fschinzel/rfisweep`.

3 Results

In this section the results from the RFI sweeps are presented. This information is organized to inform observers preparing S band observations on minimizing the impact of satellite interference.

[1]`https://github.com/caseyjlaw/jupyter-notebooks/blob/master/vlass/VLASS%20RFI.ipynb`
[2]`https://github.com/demorest/sdmpy/tree/master/sdmpy`

3.1 Peak Power

Fig. 3 provides an overview of the peak visibility amplitude levels across frequency and time for the entire data base. Fig. 4 presents a spectogram for the entire observation. From both plots the horizon-to-horizon pattern is immediately evident as well as the dominant active satellite bands at both ends of the 2–4 GHz frequency range. Figs. 5 – 20 provide a spatial view of interference broken down into the 16 spectral windows.

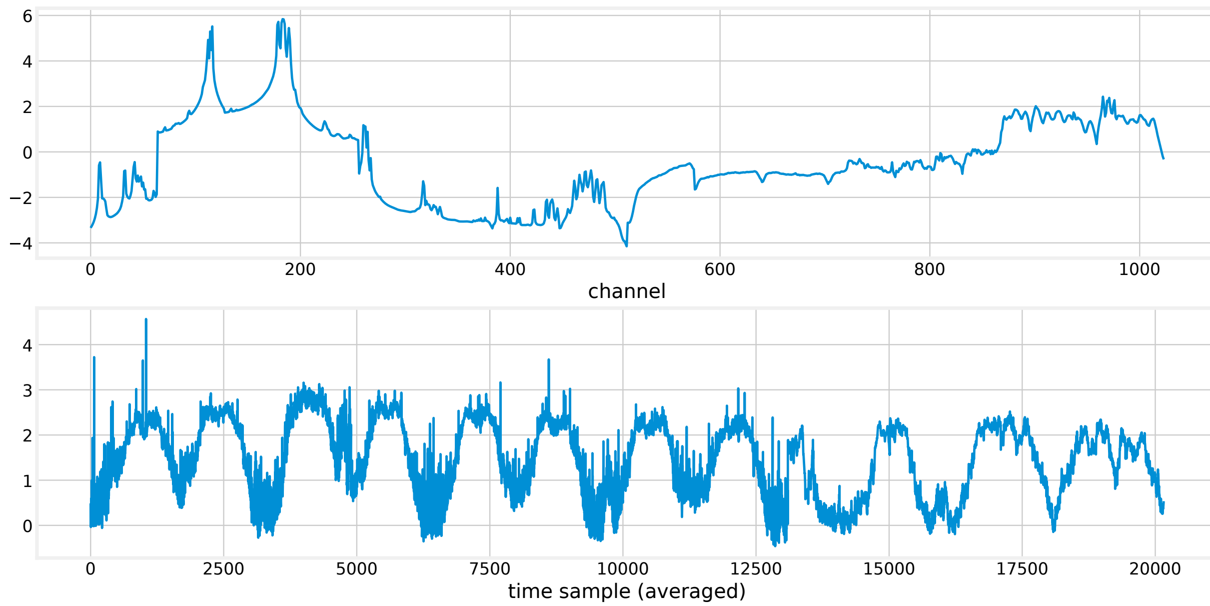

Figure 3: The top panel shows the per-channel-peak visibility amplitudes across the 2–4 GHz band. The bottom panel shows the peak amplitudes across time for the same band. Both plot amplitude scaling are logarithmic.

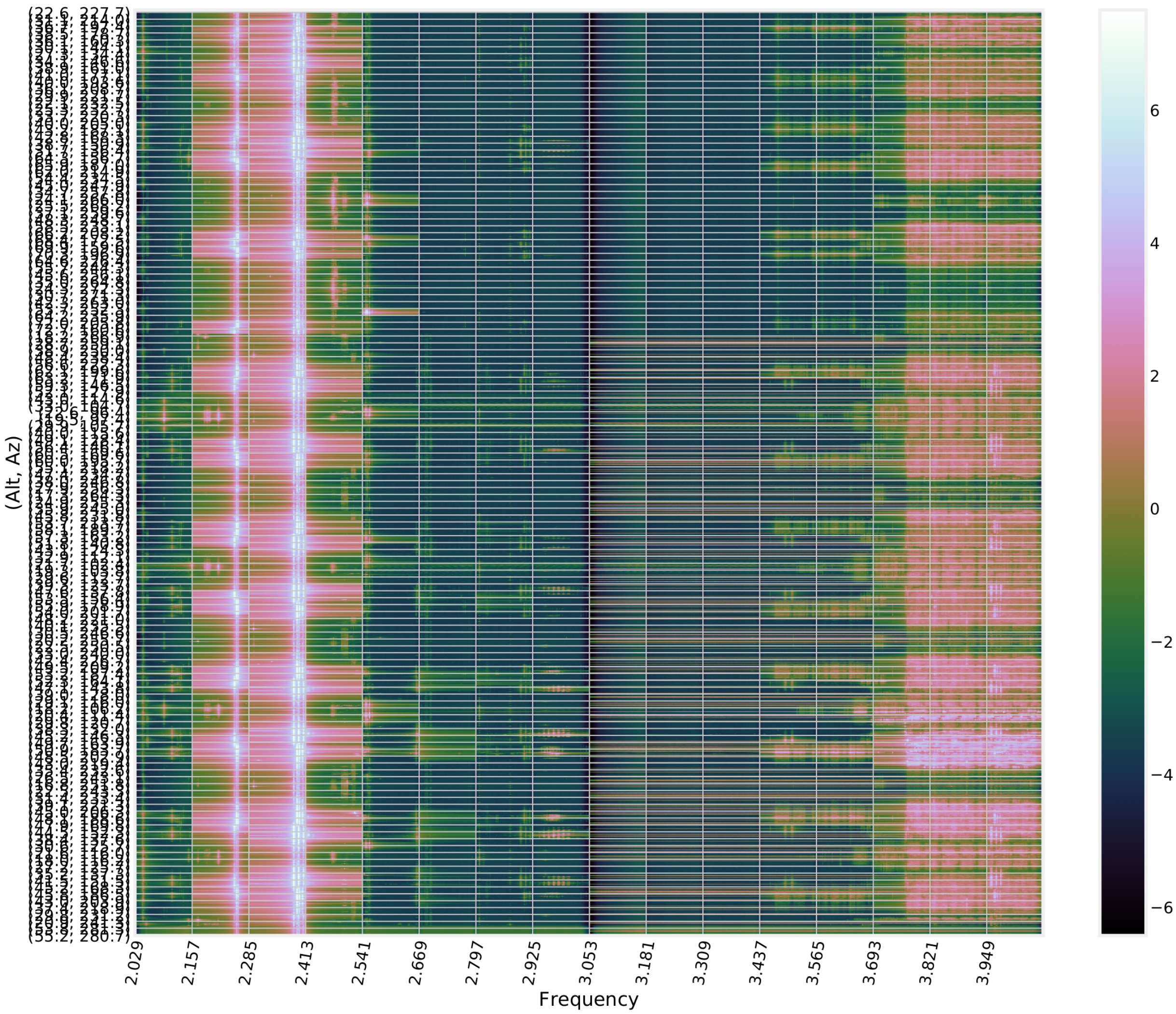

Figure 4: Spectogram of peak visibility amplitudes. The scaling is logarithmic.

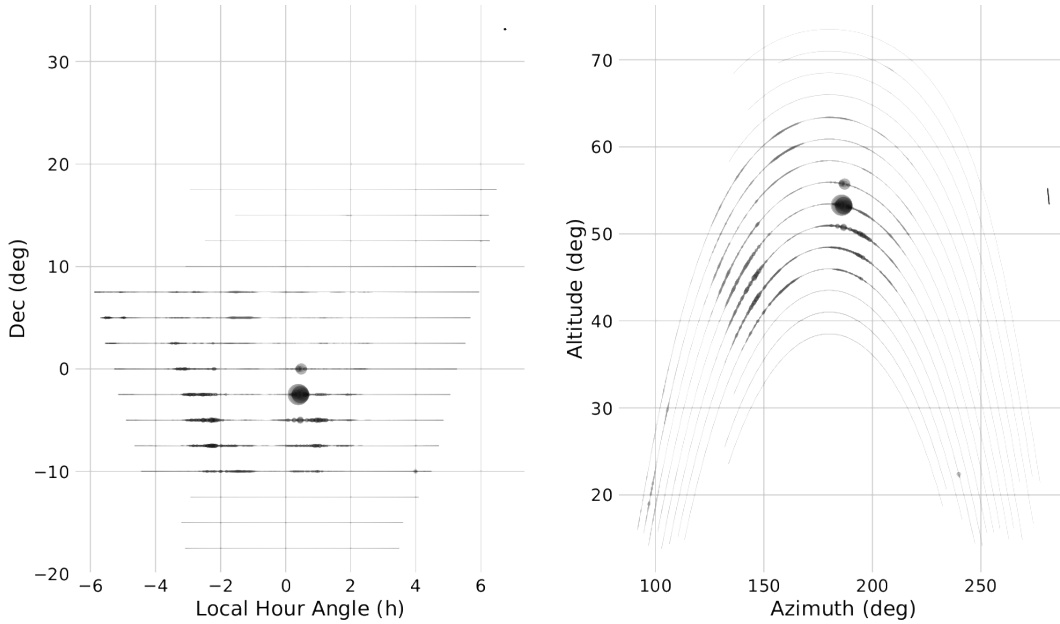

Figure 5: Spatial distribution of peak visibility amplitudes for a center frequency of 2.029 GHz and a spectral window bandwidth of 128 MHz. The left panel shows the peak visibility values plotted for declination against hour angle, while the right hand plot shows the same data in an altitude/elevation against azimuth plot. The point sizes are logarithmically scaled against the peak amplitude value across all spectral windows and pointing locations. The points at +33° declination correspond to the pointing at 3C 48 from the first dataset.

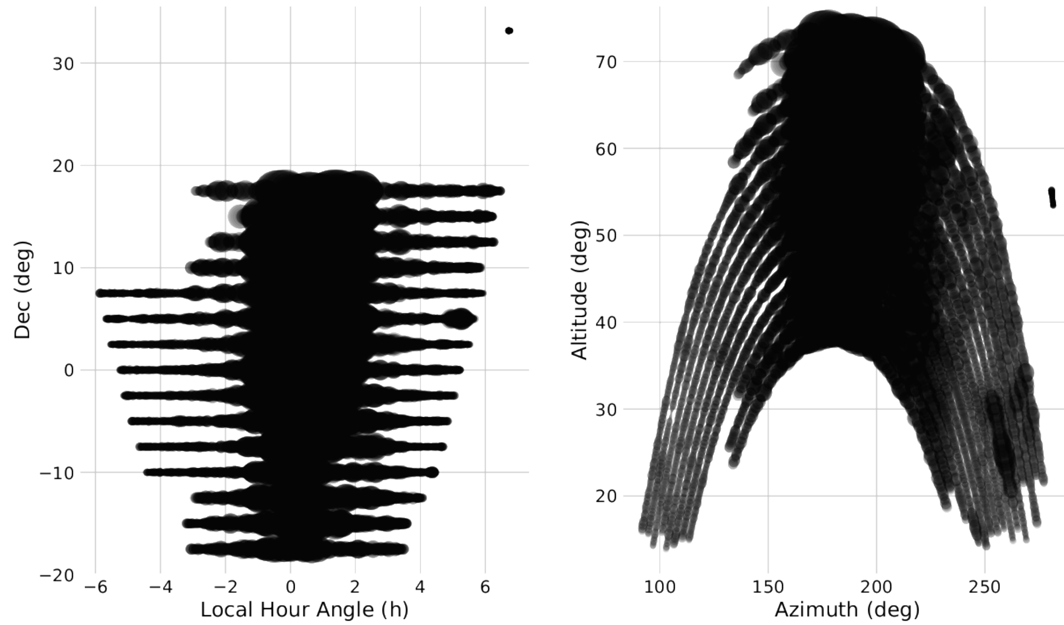

Figure 6: Sky distribution of peak visibility amplitudes similar to Fig. 5 for the spectral window with a center frequency of 2.157 GHz.

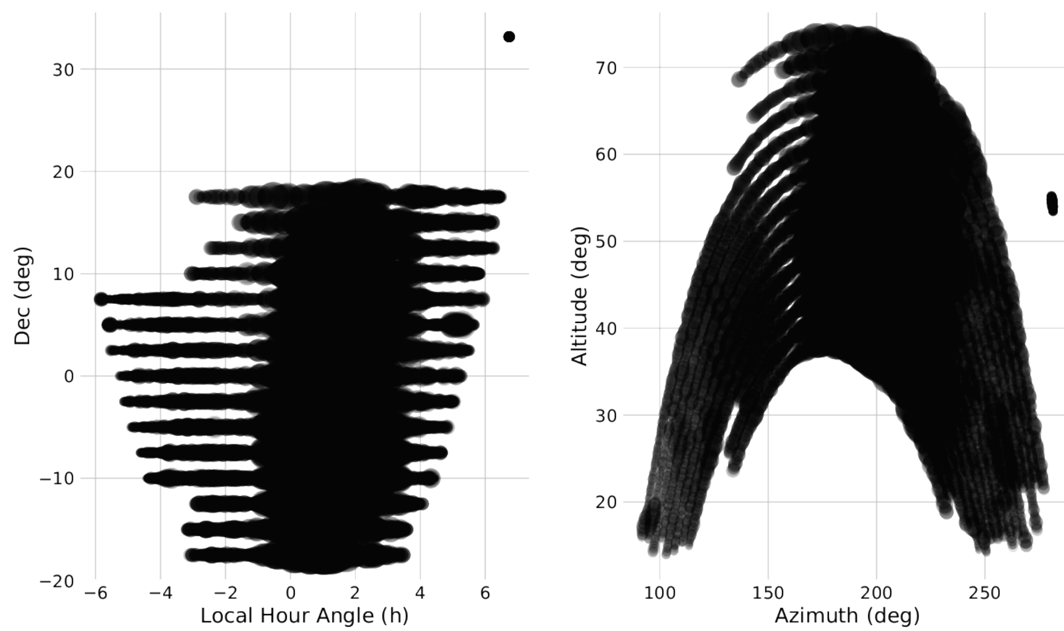

Figure 7: Sky distribution of peak visibility amplitudes similar to Fig. 5 for the spectral window with a center frequency of 2.285 GHz.

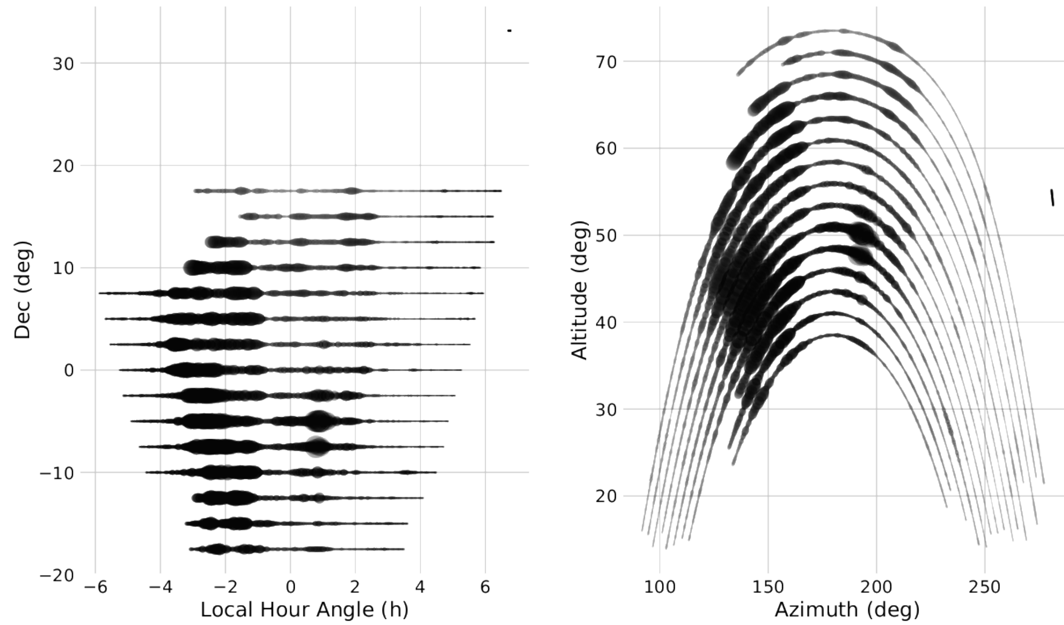

Figure 8: Sky distribution of peak visibility amplitudes similar to Fig. 5 for the spectral window with a center frequency of 2.413 GHz.

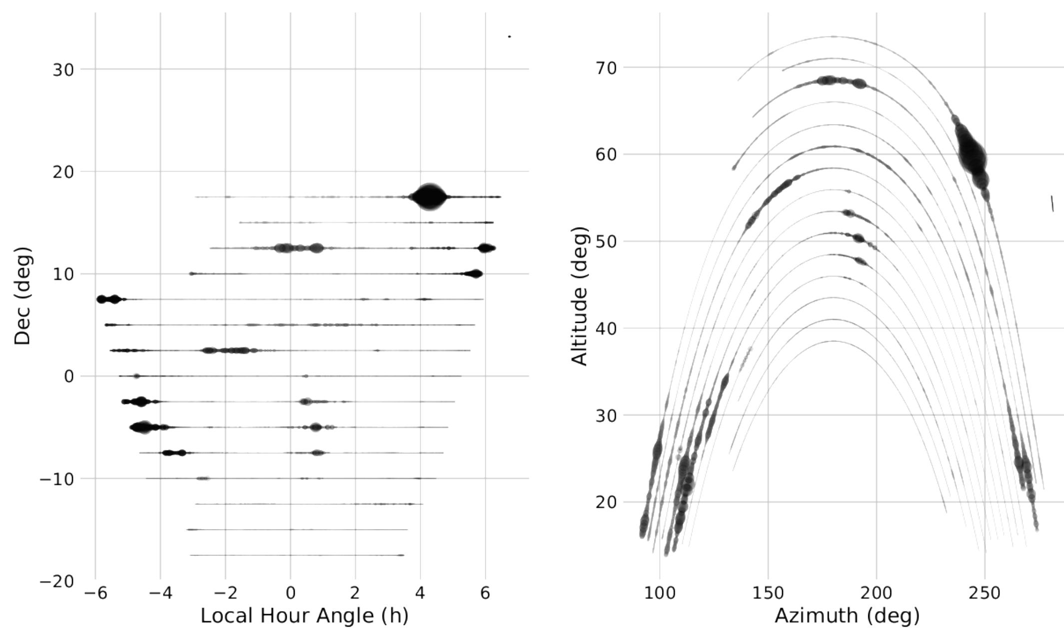

Figure 9: Sky distribution of peak visibility amplitudes similar to Fig. 5 for the spectral window with a center frequency of 2.541 GHz.

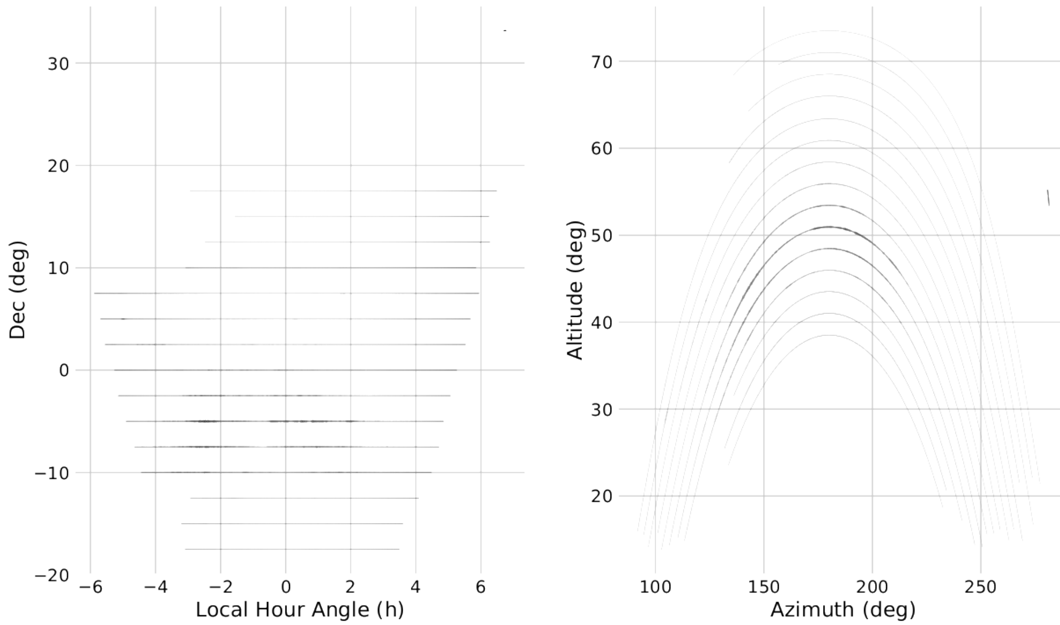

Figure 10: Sky distribution of peak visibility amplitudes similar to Fig. 5 for the spectral window with a center frequency of 2.669 GHz.

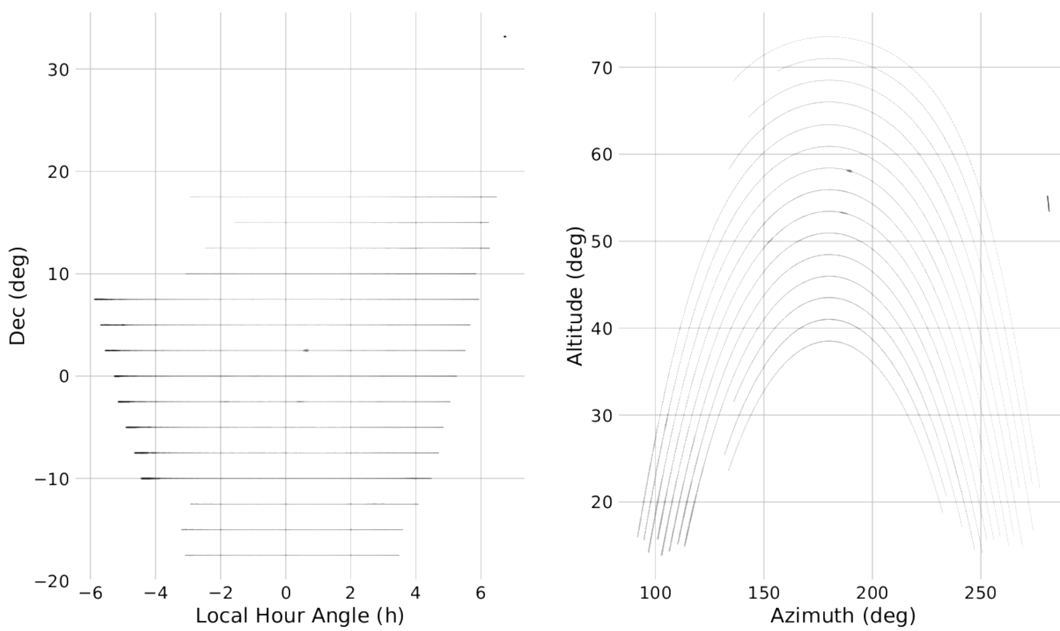

Figure 11: Sky distribution of peak visibility amplitudes similar to Fig. 5 for the spectral window with a center frequency of 2.797 GHz.

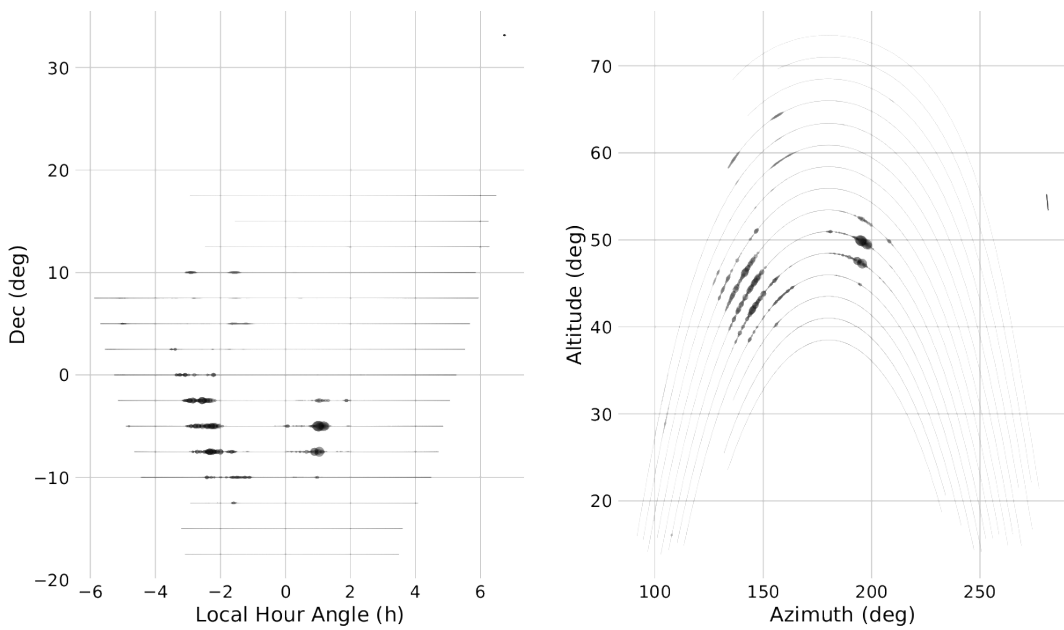

Figure 12: Sky distribution of peak visibility amplitudes similar to Fig. 5 for the spectral window with a center frequency of 2.925 GHz.

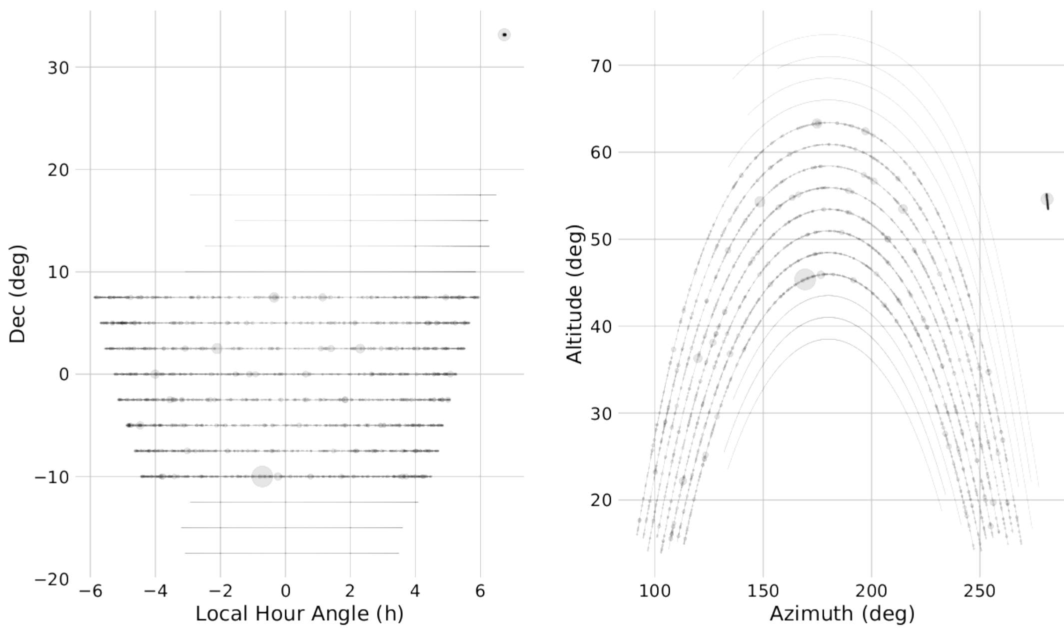

Figure 13: Sky distribution of peak visibility amplitudes similar to Fig. 5 for the spectral window with a center frequency of 3.053 GHz.

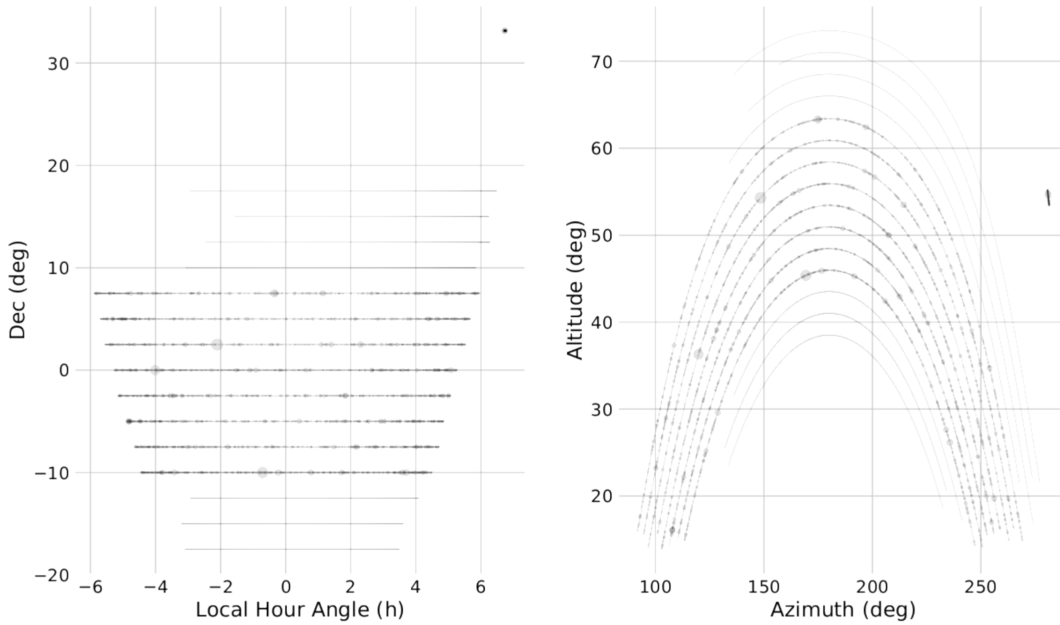

Figure 14: Sky distribution of peak visibility amplitudes similar to Fig. 5 for the spectral window with a center frequency of 3.181 GHz.

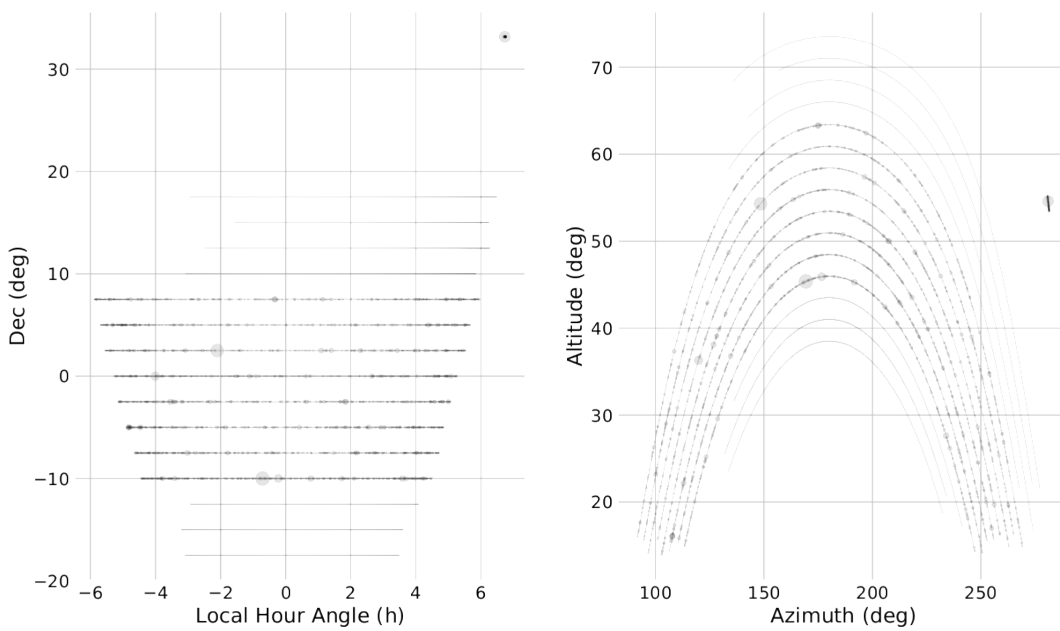

Figure 15: Sky distribution of peak visibility amplitudes similar to Fig. 5 for the spectral window with a center frequency of 3.309 GHz.

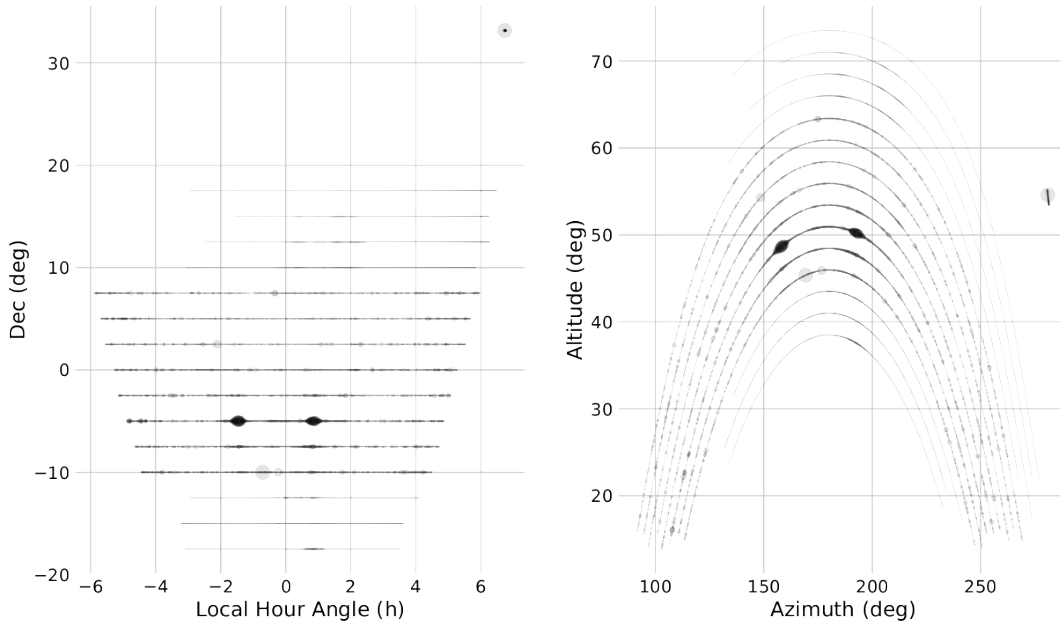

Figure 16: Sky distribution of peak visibility amplitudes similar to Fig. 5 for the spectral window with a center frequency of 3.437 GHz.

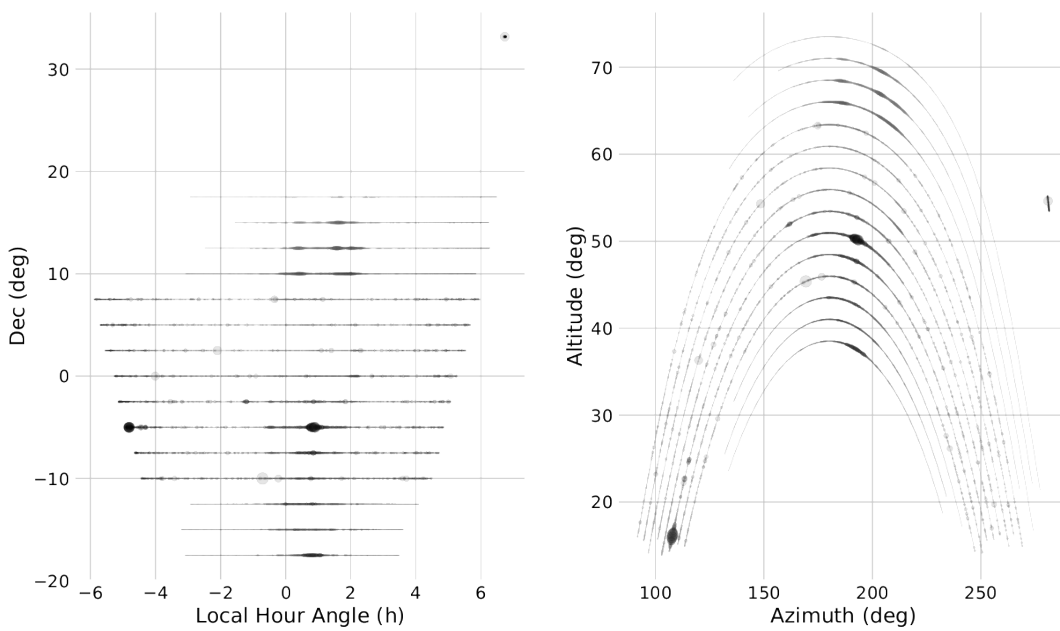

Figure 17: Sky distribution of peak visibility amplitudes similar to Fig. 5 for the spectral window with a center frequency of 3.565 GHz.

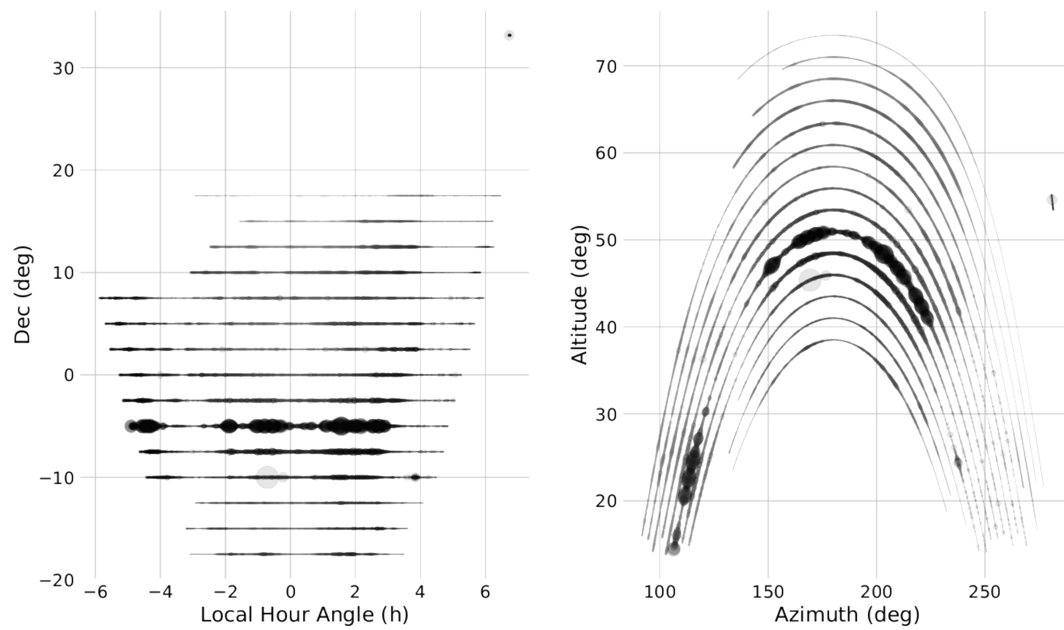

Figure 18: Sky distribution of peak visibility amplitudes similar to Fig. 5 for the spectral window with a center frequency of 3.693 GHz.

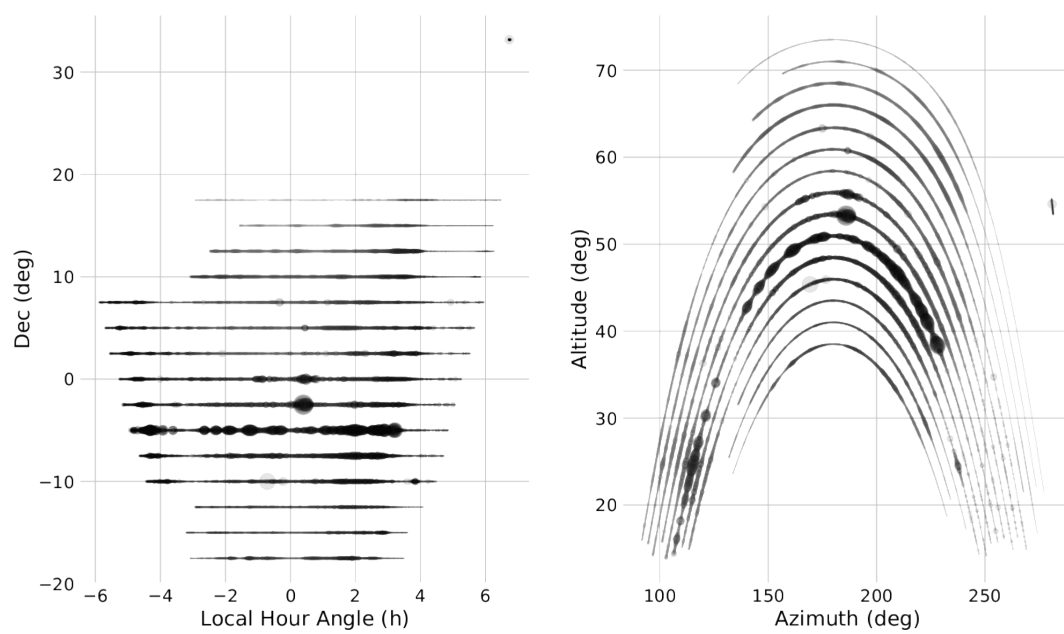

Figure 19: Sky distribution of peak visibility amplitudes similar to Fig. 5 for the spectral window with a center frequency of 3.821 GHz.

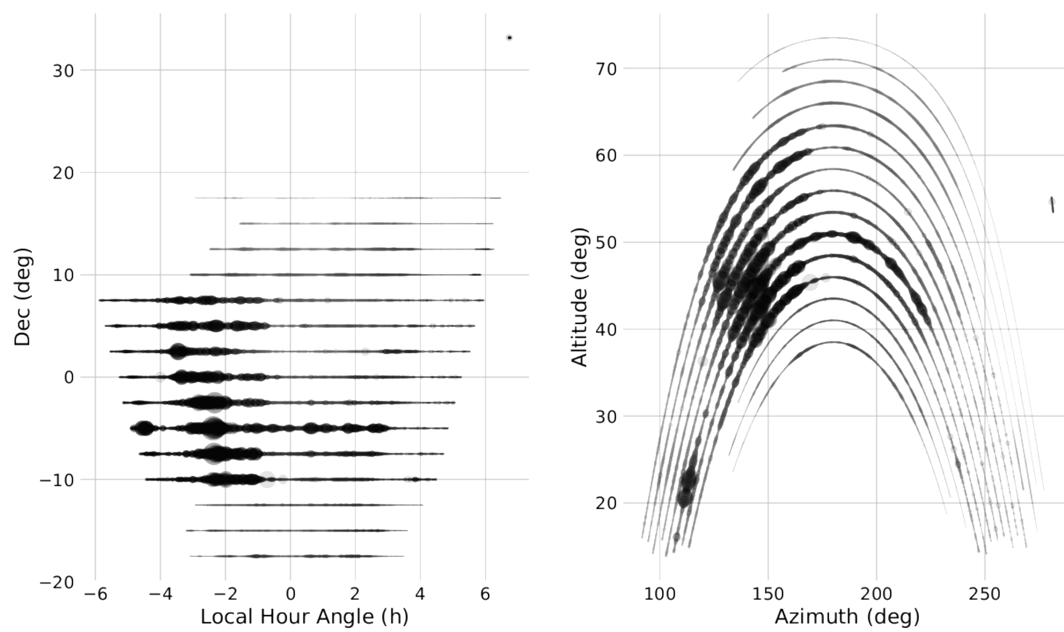

Figure 20: Sky distribution of peak visibility amplitudes similar to Fig. 5 for the spectral window with a center frequency of 3.949 GHz.

3.2 Switched Power

The switched power system of the VLA provides an estimate for gain compression of the receive system, thus indicating a deviation from gain linearity. A detailed discussion of gain compression in the presence of narrow band interference can be found here: [Perley & Hayward (2007)]. A discussion of issues regarding Pdiff compression of the VLA system can be found here: [Morris (2014)]. The Pdiff value corresponds to the difference between a noise source added to the sky signal in the receive path and the absence of it. Theoretically, a change in the Pdiff value indicates the presence of gain compression, thus we can use it to evaluate satellite interference on the receive system compared to the peak visibility amplitudes. In the presence of gain compression the observed visibility amplitudes cannot be linearly transferred, thus the error in absolute and relative flux density calibration increases following a given transfer function. The subject of this transfer function is a matter of ongoing investigation.

The switched power system is highly vulnerable to interference. Thus for further analysis of switched power spectral windows are only selected where the satellite interference is the lowest. This excluded 5 spectral windows from the lower baseband and 3 from the upper baseband, with center frequencies of 2.157, 2.285, 2.413, 2.669, 2.797, 3.693, 3.821, and 3.949 GHz. In Figures 21 – 24 the deviation of the normalized Pdiff value as a function of declination and hour angle are shown for each of the remaining spectral windows and each polarization.

In general, satellite interference is most dominant in the lower baseband, where only three spectral windows are not affected. In the upper baseband the situation is reversed, with only three spectral windows regularly affected by interference. The power levels from interference are highest in the lower baseband and left circular polarization. In most cases the Pdiff values between spectral windows are in good agreement, and in the presence of interference indicate that compression is present across the entire baseband. There is no evidence that only individual spectral windows are compressed. Finally, Figs. 25 – 28 show similar plots of Pdiff compression, however for better readability the data is binned in three categories, $> 1\%$ compression (green), $> 10\%$ compression (orange), and $> 20\%$ compression (red).

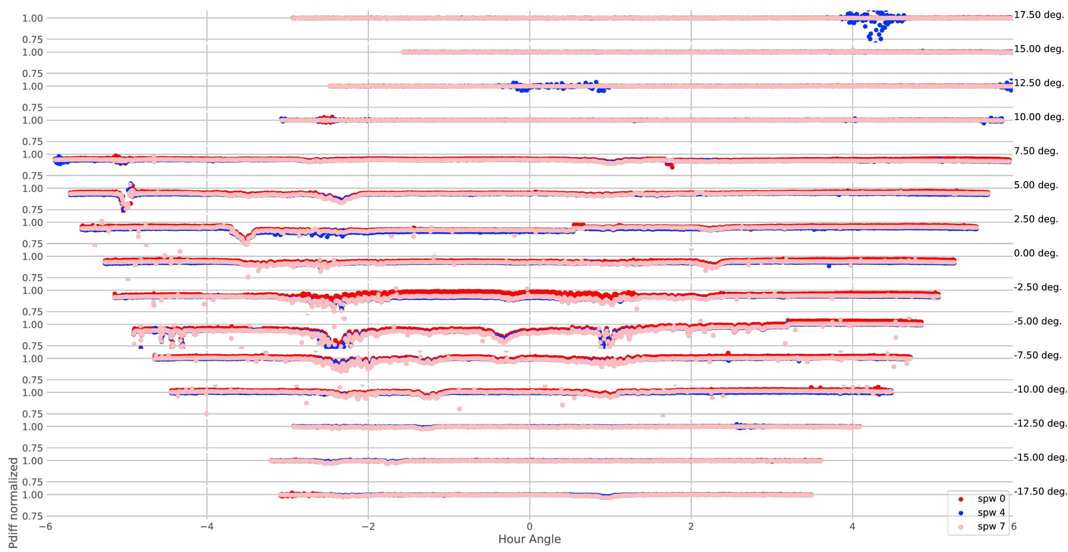

Figure 21: Pdiff values for spectral windows in the lower baseband and right circular polarization least affected by interference. Center frequencies of spectral windows are in increasing order of numbering: 2.029, 2.541, and 2.925 GHz.

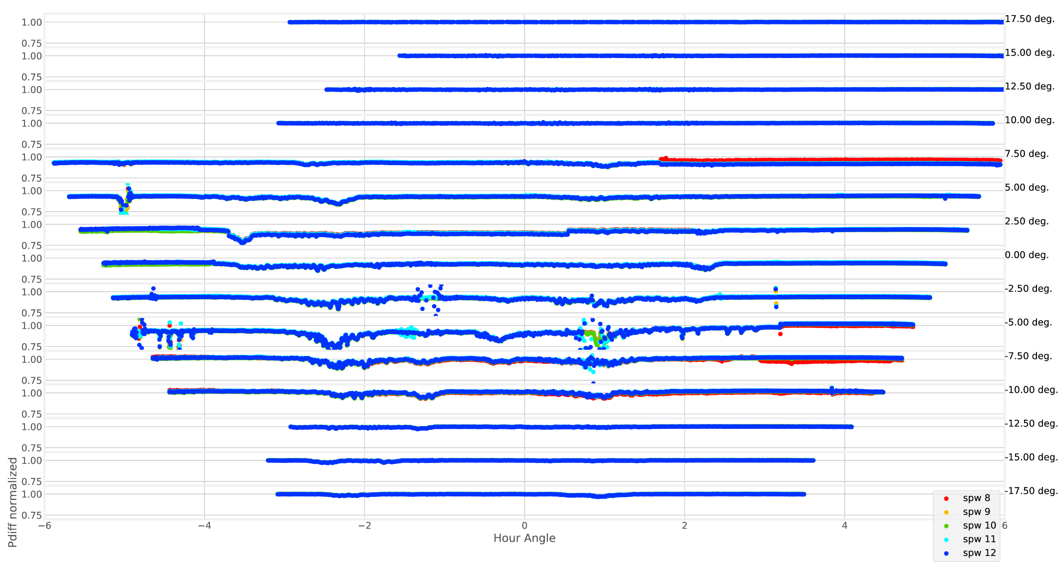

Figure 22: Pdiff values for spectral windows in the upper baseband and right circular polarization least affected by interference. Center frequencies of spectral windows are in increasing order of numbering: 3.053, 3.181, 3.309, 3.437, and 3.565 GHz.

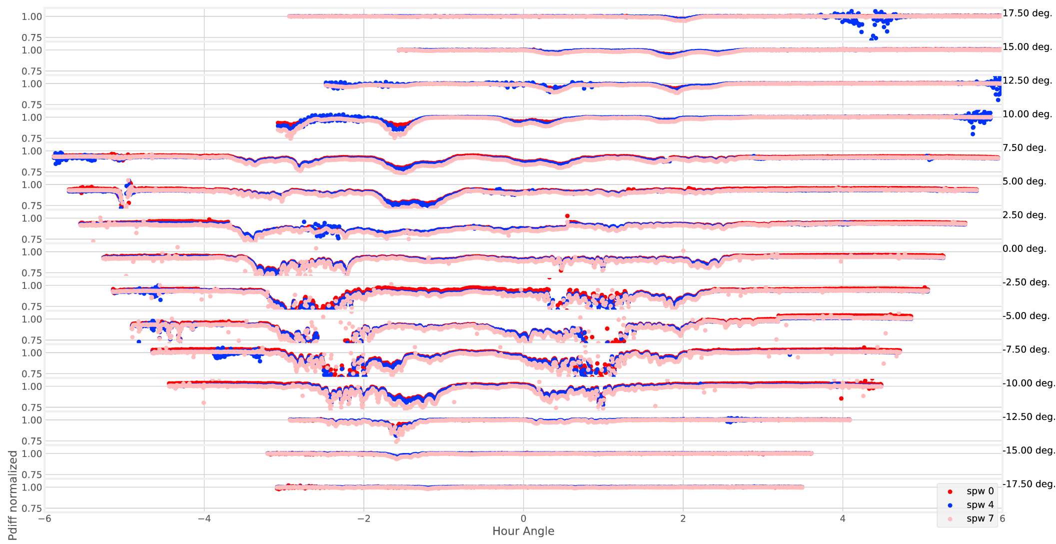

Figure 23: Pdiff values for spectral windows in the lower baseband and left circular polarization least affected by interference. Center frequencies of spectral windows are in increasing order of numbering: 2.029, 2.541, and 2.925 GHz.

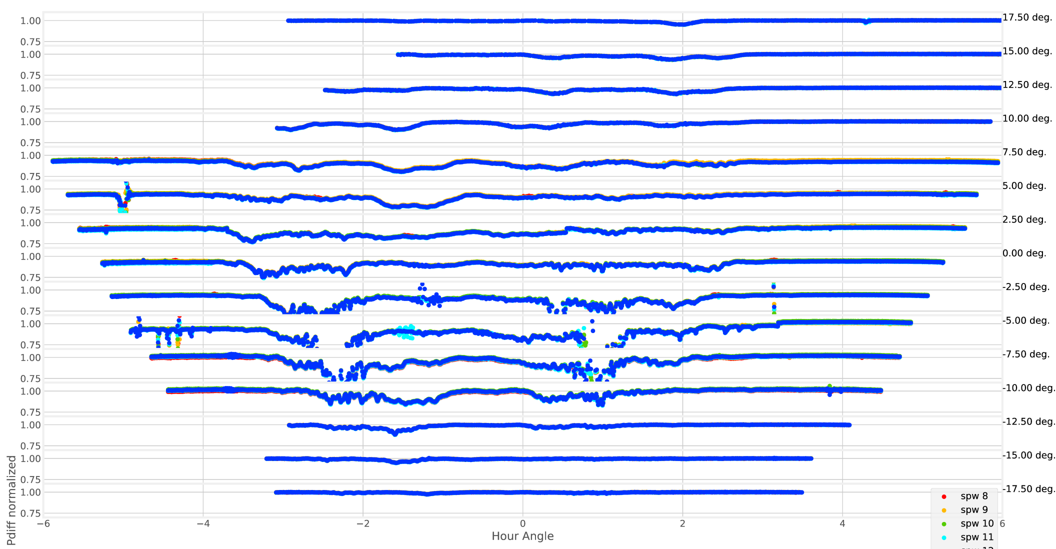

Figure 24: Pdiff values for spectral windows in the upper baseband and left circular polarization least affected by interference. Center frequencies of spectral windows are in increasing order of numbering: 3.053, 3.181, 3.309, 3.437, and 3.565 GHz.

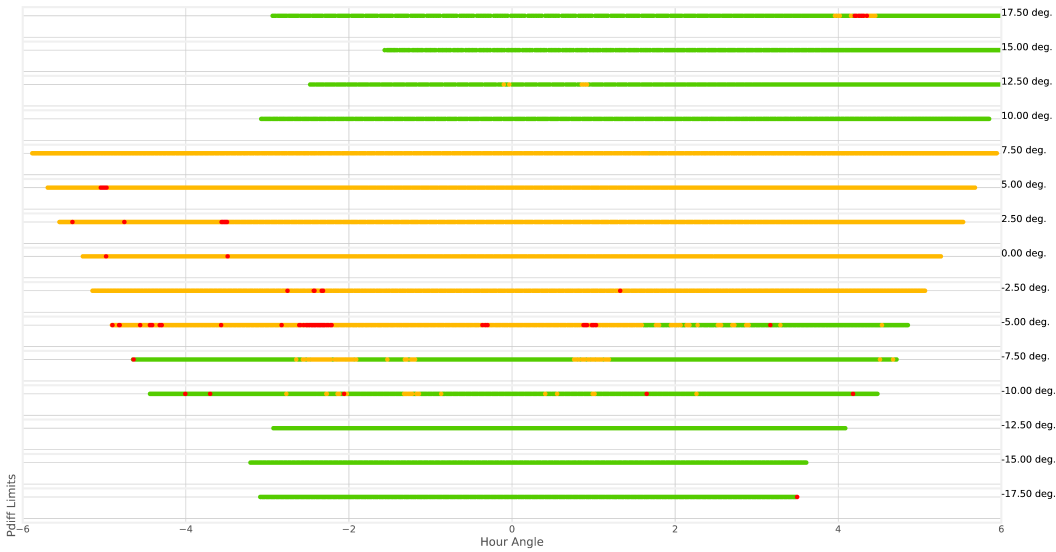

Figure 25: Pdiff values averaged across interference free spectral windows for spectral windows in the lower baseband and right circular polarization. The color coding correspond to green for <5% Pdiff compression, orange for > 5% – < 20% Pdiff compression, and red for Pdiff compression >20%.

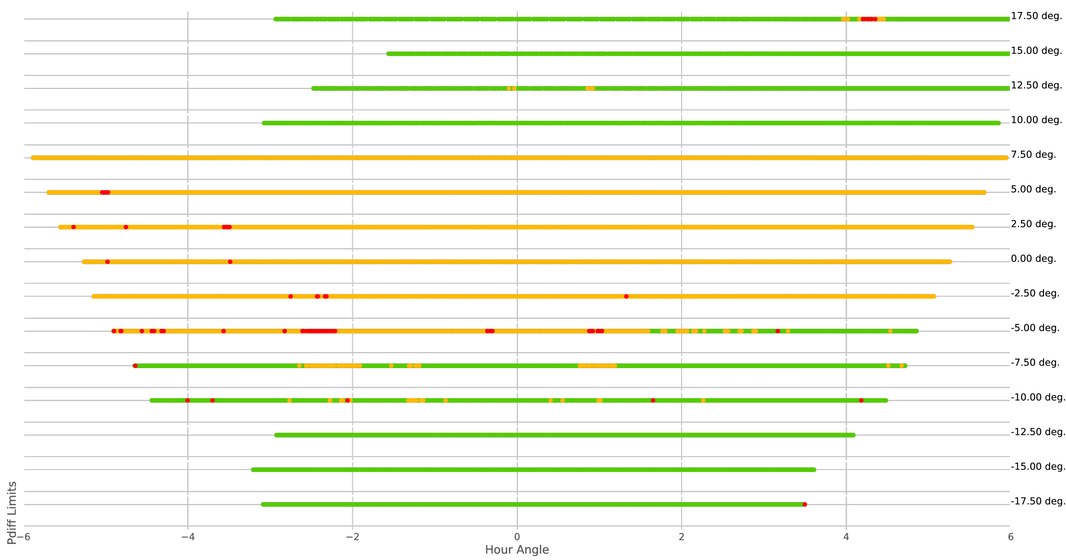

Figure 26: Pdiff values averaged across interference free spectral windows for spectral windows in the upper baseband and right circular polarization. The color coding correspond to green for <5% Pdiff compression, orange for > 5% – < 20% Pdiff compression, and red for Pdiff compression >20%.

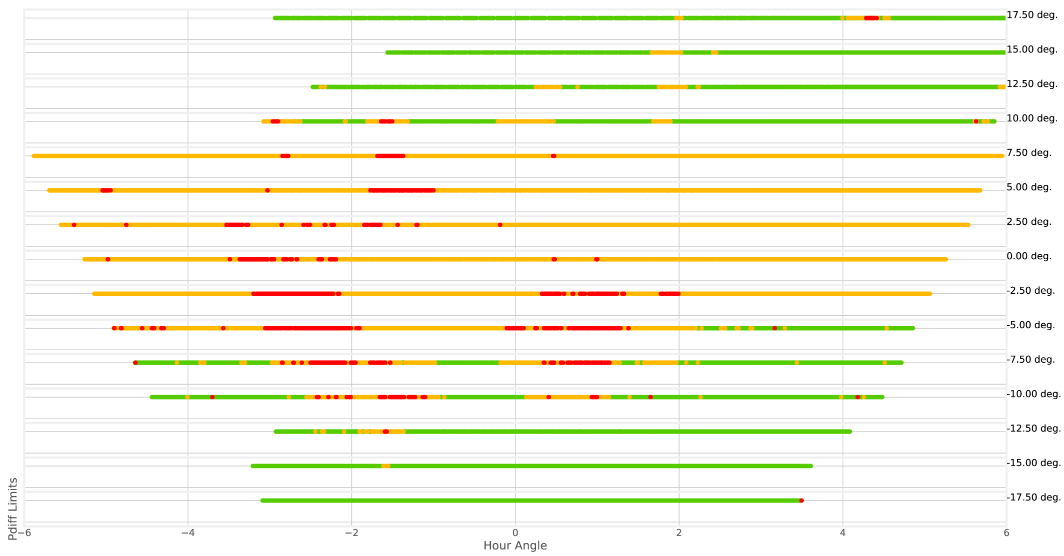

Figure 27: Pdiff values averaged across interference free spectral windows for spectral windows in the lower baseband and left circular polarization. The color coding correspond to green for <5% Pdiff compression, orange for > 5% – < 20% Pdiff compression, and red for Pdiff compression >20%.

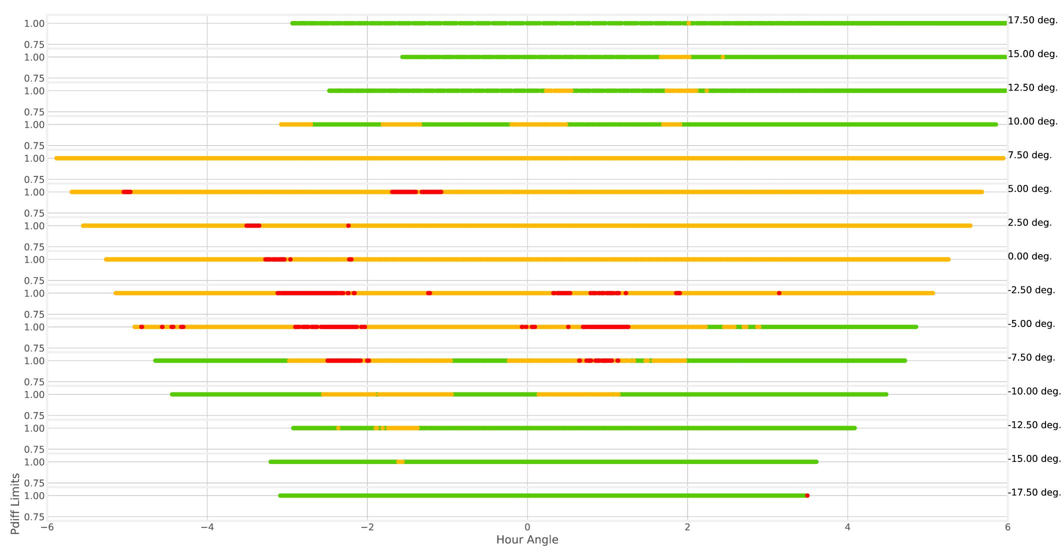

Figure 28: Pdiff values averaged across interference free spectral windows for spectral windows in the upper baseband and left circular polarization. The color coding correspond to green for <5% Pdiff compression, orange for > 5% – < 20% Pdiff compression, and red for Pdiff compression >20%.

3.3 Recommendations for Observations

The Pdiff compression plots from the previous section are now condensed to a single worst case scenario, which is recommended for scheduling decisions. Similar to Figures 25 – 28, Fig. 29 shows the minimum Pdiff values across RFI-free spectral windows and polarizations. Fig. 30 shows the unbinned minimum Pdiff values for a single declination of $-5°$, which is closest to the geostationary satellite belt. This illustrates the most severe case of S-band satellite interference for any part of the sky. The observed Pdiff compression is around 10–20% at most hour angles, and only drops when pointing toward the Pacific at hour angles > 3 hours. The observed compression is expected to affect reliability of amplitude calibration at times of observed Pdiff compression. It is highly recommended to avoid observing sources at declinations and hour angles that show Pdiff compression >5%. If observations with up to 20% Pdiff compression cannot be avoided, compression might be correctable during post processing. This occurs primarily around -0.5 ± 0.25 and 1.0 ± 0.25 hour angles at $-5°$ declination. To summarize and quantify areas of 5%–20% compression and $> 20\%$, Table 2 parametrizes Fig. 25.

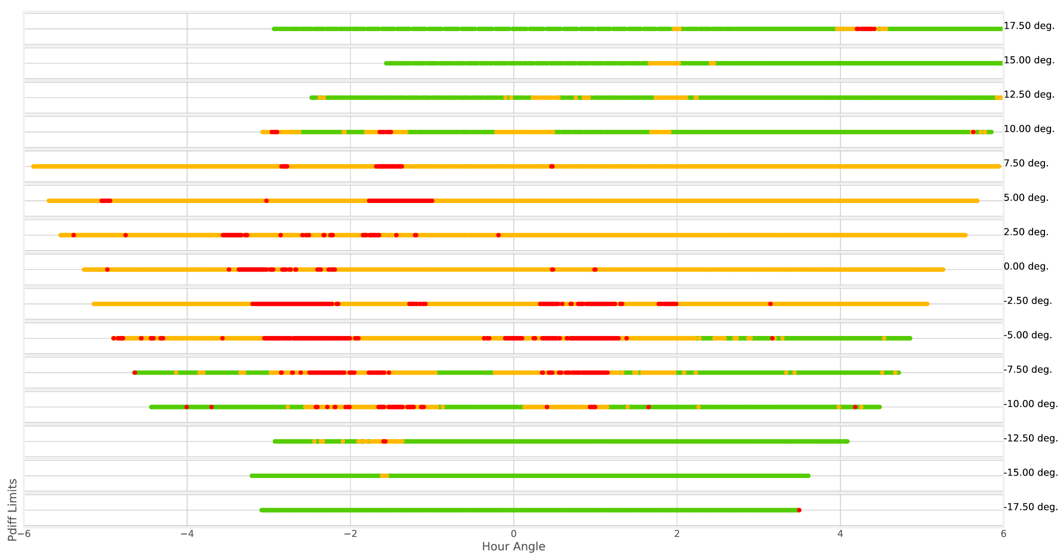

Figure 29: Minimum Pdiff values averaged across interference free spectral windows and both circular polarizations. The color coding correspond to green for <5% Pdiff compression, orange for $> 5\%$ and $< 20\%$ Pdiff compression, and red for Pdiff compression >20%.

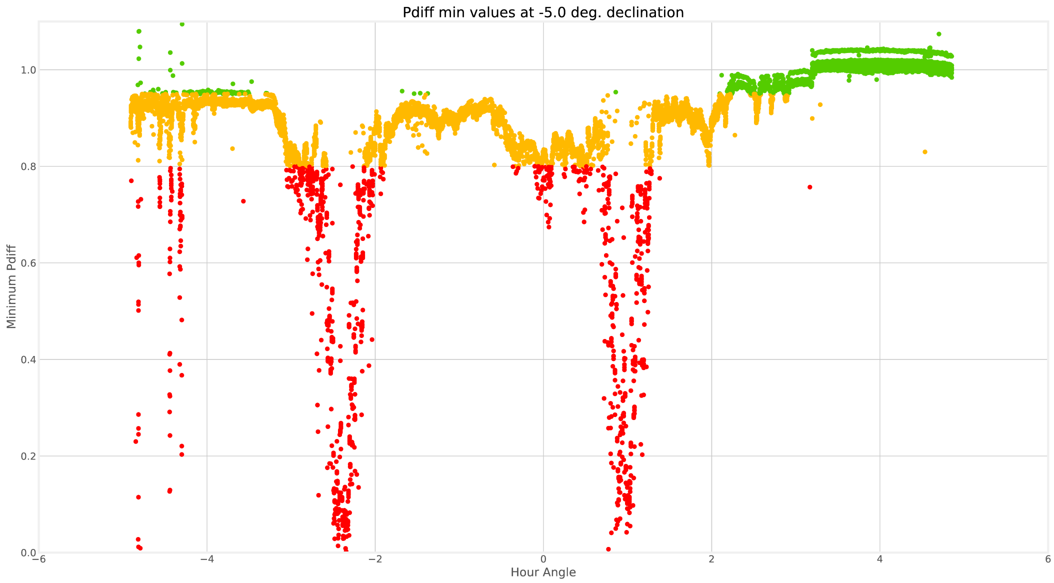

Figure 30: Minimum Pdiff values for interference free spectral windows across both polarizations. The color coding correspond to three different bins, green for < 5% Pdiff compression, orange for > 5% and < 20% Pdiff compression, and red for Pdiff compression >20%.

Table 2: Summary of hour angle ranges within which the normalized Pdiff value was observed to be compressed above 5% tabulated by declination range and two Pdiff compression levels, > 5% and > 20%. The arrow indicates interference likely to extend beyond the observed hour angle.

Declination	Pdiff compression	
	> 5% Hour Angle	> 20% Hour Angle
(deg.)	(h)	(h)
17.5	1.91 – 2.05	-
15.0	1.64 – 2.02	-
	2.41 – 2.46	-
12.5	← -2.49 – -1.25	-
	0.22 – 0.56	-
	1.72 – 2.12	-
	2.22 – 2.25	-
10.0	← -3.10 – -2.61	-3.00 – -2.86
	-1.81 – -1.31	-1.66 – -1.46
	-0.23 – 0.48	-
	1.65 – 1.93	-

7.5	← -5.90 – 5.98 →	-2.86 – -2.75
	.	-1.69 – -1.35
5.0	.	-5.06 – -4.93
	.	(non-geostationary)
	← -5.71 – 5.71 →	-3.01
	.	-1.79 – -0.98
2.5	.	-3.57 – -3.32
	.	-3.29 – -3.26
	.	-2.58 – -2.50
	← -5.58 – 5.56 →	-2.33 – -2.31
	.	-2.25 – -2.20
	.	-1.85 – -1.80
	.	-1.77 – -1.64
0.0	.	-3.38 – -2.92
	.	-2.86 – -2.64
	← -5.28 – 5.29 →	-2.43 – -2.34
	.	-2.28 – -2.16
	.	0.47 – 0.48
	.	0.98 – 1.00
-2.5	.	-3.17 – 2.13
	.	-1.28 – -1.06
	← -5.16 – 5.10 →	0.29 – 1.35
	.	1.75 – 2.02
	.	3.15
-5.0	.	-4.90
	.	-4.85 – -4.83
	.	-4.82 – -4.80
	.	-4.79 – -4.78
	.	-4.56 – -4.55
	.	-4.45 – -4.40
	← -4.90 – 2.26	-4.33 – -4.29
	.	-3.07 – -1.89
	.	-0.37 – -0.26
	.	-0.14 – -0.12
	.	0.23 – 0.27
	.	0.34 – 0.57
	.	0.63 – 1.42
	2.45 – 2.59	-
	2.69 – 2.74	-
	2.86 – 2.90	-
-7.5	.	-2.85 – -2.84

	.	-2.71 – -2.70
	.	-2.61
	-2.99 – -0.93	-2.51 – -2.07
	.	-2.01 – -1.94
	.	-1.78 – -1.58
	.	-1.53
	-0.25 – 2.00	0.31 – 1.16
-10.0	.	-2.42 – -2.40
	.	-2.28
	.	-2.19 – -2.18
	-2.58 – -0.91	-2.06 – -2.00
	.	-1.66 – -1.59
	.	-1.53 – -1.36
	.	-1.30 – -1.22
	.	-1.13 – -1.09
	.	0.40
	0.11 – 1.17	0.93 – 1.00
	.	1.65
-12.5	-2.44	-
	-2.37 – -2.33	-
	-2.09	-
	-1.96 – -1.86	-
	-1.84 – -1.79	-
	-1.76 – -1.35	-1.59 – -1.57
-15.0	-1.62 – -1.55	-
-17.5	-	-

4 Summary & Conclusions

Radio interference from satellites (geo- and non-geostationary) transmitting at S-band frequency as seen from the VLA can have a significant impact on observations, especially when observing between 7.5° and −10.0° declination. Care should be taken to avoid the highest impact areas that cause Pdiff compression at levels > 20%. In general the frequency range 2.093 – 2.477 GHz is heavily affected by interference for most pointing directions, while geostationary satellite interference is primarily contained to frequencies 3.100 - 4.200 GHz in the C-band allocation of the satellite downlink band plan.

Satellite interference is not limited to S band but is also a concern at C, X, and Ku-band. A similar survey would provide additional information for interference avoidance and provide a snapshot of the severity of satellite emission in each of the bands.

Acknowledgements

I thank Casey Law and Paul Demorest for sharing their python code for reading SDMs and for creating visualization which was used as starting point for the analysis. I also thank Vivek Dhawan and Josh Marvil for useful discussions, especially concerning switched power. I thank Alan Erickson for his feedback on the first full draft.

References

[Perley & Hayward (2007)] R.Perley & B. Hayward 2007 The Effect of Amplifier Compression by Narrowband RFI on Radio Interferometer Imaging EVLA Memo #110

[Morris (2014)] K. Morris 2014 Gain and Pdiff Compression in the EVLA IF Signal Path: Strategies for Identification and Mitigation EVLA Memo #184

[UCS (2018)] UCS Satellite Database `https://www.ucsusa.org/nuclear-weapons/space-weapons/satellite-database?_ga=2.223516827.1657936800.1517243136-1030239748.1517243136#.W05oAq2zDNd`

Revision History

Revision	Date	Author(s)	Description
2.0	2018-07-20	Frank Schinzel	final
1.1	2018-07-17	Frank Schinzel	revised draft
1.0	2017-12-05	Frank Schinzel	first full draft